Spontaneous and evoked synaptic rewiring in the neonatal neocortex

Jean-Vincent Le Bé and Henry Markram*

Brain Mind Institute, Ecole Polytechnique Fédérale de Lausanne, CH-1015 Lausanne, Switzerland

Communicated by Michael M. Merzenich, University of California, San Francisco, CA, July 3, 2006 (received for review March 21, 2006)

The local microcircuitry of the neocortex is structurally a tabula rasa, with the axon of each pyramidal neuron having numerous submicrometer appositions with the dendrites of all neighboring pyramidal neurons, but is functionally highly selective, with synapses formed onto only a small proportion of these targets. This design leaves a vast potential for the microcircuit to rewire without extensive axonal or dendritic growth. To examine whether rewiring does take place, we used multineuron patch-clamp recordings on 12- to 14-day-old rat neocortical slices and studied long-term changes in synaptic connectivity within clusters of neurons. We found pyramidal neurons spontaneously connecting and disconnecting from each other and that exciting the slice with glutamate greatly increases the number of new connections established. Evoked emergence of new synaptic connections requires action potential activity and activation of metabotropic glutamate receptor 5, but not NMDA receptor or group II or group III metabotropic glutamate receptor activation. We also found that it is the weaker connections that are selectively eliminated. These results provide direct evidence for spontaneous and evoked rewiring of the neocortical microcircuitry involving entire functional multisynaptic connections. We speculate that this form of microcircuit plasticity enables an evolution of the microcircuit connectivity by natural selection as a function of experience.

plasticity | pyramidal neurons | synaptic connections

Synapses are formed and pruned during development (1–3), but how is a neuron selected for or against becoming or remaining an output target of a presynaptic cell? Recent studies made an important step toward understanding target selection by showing that the axon of a pyramidal neuron approaches, at a submicrometer distance, the dendrites of every neighboring pyramidal neuron multiple times without any structural bias toward those with which synaptic connections are formed (4–6). This finding raised the possibility that the microcircuit could be in an all-to-all "readiness" to switch rapidly on and off connections between neurons in a form of rewiring plasticity without the axon or the dendrite growing toward a new target. Rapid proliferation of spines in slices (within the first 2 h after slicing) has been shown in young and adult rat hippocampus (7), but whether new functional connections are being formed and eliminated is not known. To determine whether the microcircuit can rewire we used the multineuron patch-clamp approach to study spontaneous and evoked changes in connectivity within small clusters of six to seven layer-5 thick tufted pyramidal neurons (TPCs) (see *Materials and Methods*). We began the experiments after a 2-h stabilization period after slicing.

Synaptic connections are easily revealed by presynaptic trains of action potentials, and averaged postsynaptic traces can detect very small events (≈10 μV) below the smallest synaptic responses typically recorded between neurons (≈50 μV) (8). Synaptic connections between TPCs are stable for many hours of recording, and no emergences or disappearances of connections have ever been observed in experiments lasting >8 h (H.M., unpublished data). This stability may be because plasticity is restricted to the scaling of existing synapses, because rewiring does not occur on such time scales, or because rewiring was prevented by the washout of the internal milieu by the patch pipette. We therefore prepared neocortical slices of the rat somatosensory cortex in the standard manner, but we patched and then repatched neurons after 12 h (see *Materials and Methods*). IR differential interference contrast microscopy allows selection of specific neurons (Fig. 1*A*) and repeated patching of the same neurons (Fig. 1*A Right*). We could further verify that the same neurons were repatched by staining the recorded cells (Fig. 1*B*; see *Materials and Methods*).

Brain slices display very little spontaneous activity under the standard conditions we use, and the slice was therefore activated with bath and local application of Na-glutamate. Periodic puffing of Na-glutamate from a patch pipette above the pyramidal cluster (50 mM, 2 s every 1 min, "Evoked 1" condition) caused similar discharges in all cells (Fig. 1*C*), which was reasonably stable for hours (Fig. 1*D*). Bath application of glutamate (100 μM, "Evoked 2" condition) brought cells rhythmically to spiking threshold (Fig. 1*E*).

Results

Spontaneous and Evoked Changes. A cluster of six to seven TPCs was typically recorded. The first recording in the experiment is referred to as "before" and the second recording, after 12 h in various conditions or 4 h with glutamate puffing, is referred to as "after." Two indices were used for quantifying the connectivity changes. The emergence index (*Ei*) is the proportion of new functionally connected pairs "after" among unconnected pairs "before," and the disappearance index (*Di*) is the proportion of existing connected pairs "before" that were not connected anymore "after." In control experiments we found that connections spontaneously emerged ($Ei = 4 \pm 1\%$, mean ± SD) (Fig. 2 *A* and *B*) and disappeared ($Di = 13 \pm 7\%$, mean ± SD) (Fig. 2 *A* and *C*), indicating that functional synaptic connections are formed and removed on the time scale of hours. Bath and periodic puff application of glutamate caused nearly a doubling of the total number of connected pairs and a >4-fold increase in the *Ei* (16 ± 3% and 14 ± 3% for Evoked 1 and Evoked 2, respectively) (Fig. 2*B*; see *Materials and Methods*), indicating that glutamate-mediated excitation strongly drives the formation of new connections. The application of glutamate did not increase the disappearance of connections. On the contrary, the trend was rather to prevent disappearances (Evoked 1: $Di = 6 \pm 4\%$), although this was not statistically significant (Fig. 2*C*). The patching procedure may also contribute some uncertainty to the significance of physiological disappearances of connections (but see *Selecting Against Weak Connections*).

Conflict of interest statement: No conflicts declared.

Abbreviations: *A*, absolute synaptic efficacy (strength); EPSP, excitatory postsynaptic potential; *Pr*, probability of release; TPC, layer-5 thick tufted pyramidal neurons; ACSF, artificial cerebrospinal fluid; TTX, tetrodotoxin; MPEP, 2-methyl-6-(phenylethynyl)pyridine; EGLU, (2*S*)-α-ethylglutamic acid; CPPG, (*RS*)-α-cyclopropyl-4-phosphonophenylglycine; *Ei*, emergence index; *Di*, disappearance index; CNQX, 6-cyano-7-nitroquinoxaline-2,3-dione; AP5, D-2-amino-5-phosphonopentanoic acid; AP3, DL-2-amino-3-phosphopropinionic acid; *CV*, coefficient of variation; mGluR, metabotropic glutamate receptor.

*To whom correspondence should be addressed. E-mail: henry.markram@epfl.ch.

www.pnas.org/cgi/doi/10.1073/pnas.0604691103

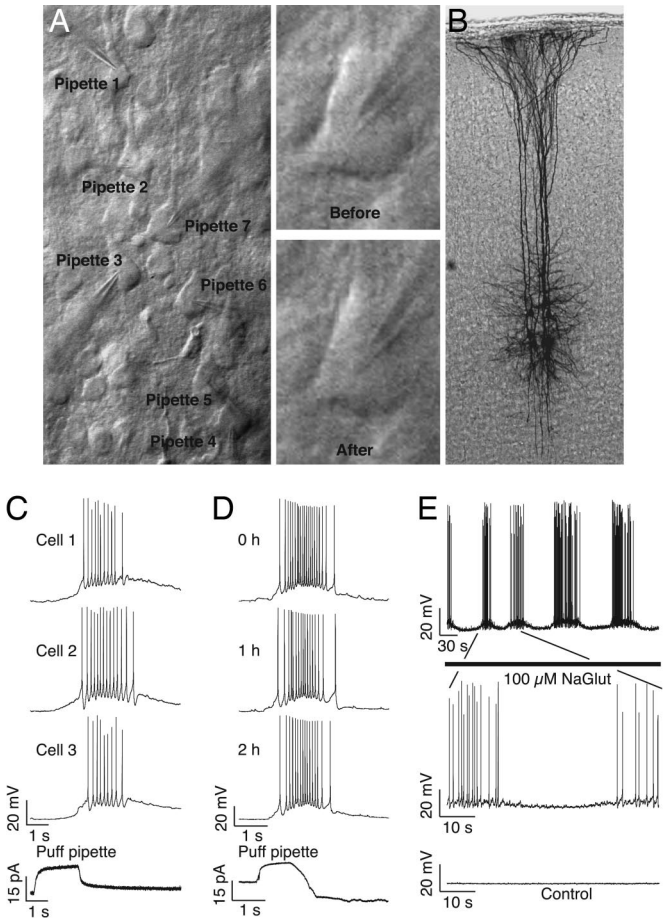

Fig. 1. Visualization and stimulation of TPC clusters. (*A*) IR differential interference contrast image of a seven-cell cluster patched. (*Right*) A neuron at first patch (''Before'') and repatched after 12 h (''After''). (*B*) Biocytin-stained cluster shows that only seven cells were patched despite the two separated sessions. (*C*) Whole-cell recordings of three of the six cells recorded while glutamate was puffed from the seventh patch pipette located ≈100 μm above the cluster (bottom trace). (*D*) Stability of the response to glutamate puffing over time. (*E*) Response of a cell to bath application of glutamate. ''Control'' shows the same time and voltage scale trace of a cell in normal ACSF.

Selecting Few Targets with Many Synapses. We also examined how neurons select a very small fraction of neurons in a microcircuit and then place multiple synapses in a distributed manner across a relatively large volume of cortical space on the chosen target neurons (8–16). For these TPCs connectivity is known to be ≈10–15% (17), and multiple synapses are involved in each connection (8, 18). We therefore examined the strength [*A* = first excitatory postsynaptic potential (EPSP) amplitude/probability of release (*Pr*)] and *Pr* (see *Materials and Methods*) of the emerging and disappearing connections recorded at the cell soma to gain some insight into the types of synaptic connections that were being formed and removed. We found that the average strength (*A*) of new connections was smaller than those of existing connections (Fig. 2*D*) [1.5 ± 0.1 mV vs. 2.4 ± 0.1 mV, mean ± SEM ($P < 0.001$), $n = 122$ multisynaptic emerged connections overall and 322 existing connections ''before''] as was the distribution of synaptic strengths with a higher number of weaker connections ($P < 0.001$, Kolmogorov–Smirnov test). The average *Pr* was also lower (Fig. 2*D*) [0.36 ± 0.01 vs. 0.45 ± 0.01, mean ± SEM ($P < 0.001$), $n = 122$ multisynaptic emerged connections overall and 322 existing connections ''before''']. The coefficient of variation (*CV*) of responses was significantly but not proportionately higher [0.70 ± 0.07 vs. 0.43 ± 0.06, mean ± SEM ($P < 0.01$), $n = 14$ and 16, Evoked 1 emerged vs. existing ''before''], requiring an assumption of a lower number of synapses per connection (*N*) to explain the magnitude of the increase in the *CV* (0.53, predicted for the same *N*; 0.70, *CV* actual; see *Materials and Methods*). Although binomial assumptions may not perfectly hold at these connections (8, 19, 20), a prediction of the number of functional release sites using binomial analysis does support new connections with fewer synapses at the time of the recording (binomial $N \approx 5$ for new connections, and $N \approx 8$ for existing ones; see *Materials and Methods*). Multisynapse connections are therefore being formed within hours, and synapses seem to have been progressively added over this time. Additions probably continue to achieve the same average number of synapses as for existing connections. The new connections also seem to begin with lower probabilities of release, which presumably increase to reach the same average as existing synapses.

Selecting Against Weak Connections. We also found that the synaptic connections that disappeared were preferentially the weaker ones [1.1 ± 0.3 mV vs. 2.4 ± 0.1 mV, $n = 24$ and 322 ($P < 0.001$)]. It could be that the patching procedure contributed to this finding, but it is more likely that such damage would affect connections randomly. These weak connections were also different from the newly emerging weak connections in that their probabilities of release were similar to those of remaining connections (0.44 ± 0.03 vs. 0.45 ± 0.01, $n = 24$ multisynaptic connections disappeared and 322 existing connections ''before'' which persisted) (Fig. 2*E*), whereas the *Pr* of new connections was lower. Thus, new weak connections do not seem to be subject to the same elimination process as existing weak connections. This could be a ''grace'' period for the new connections to be tested in the circuit, and only around the time that the average *Pr* of new connections reaches the average in the population do connections become subject to elimination. Such a process of delayed selection against the weakest connections may explain how the microcircuit ends up with a small and selected fraction of neurons wired with multisynapse connections.

The time course of emergence of new connections, ''maturation'' before elimination, and the elimination process will need to be exhaustively studied in the future, but we did some preliminary experiments after 4 h and found that the evoked emergences with 4 h already tended to exceed the spontaneous emergences after 12 h (6 ± 2%, $n = 140$ pairs in six clusters). Although this increase was not significant, a linear fit through 0, 4, and 12 h was 99.6% accurate, yielding an estimated rate of 1.2% newly connected pairs per hour after excitation (data not shown). One multisynapse connection had disappeared over all of the experiments performed in 4 h (>29 connected pairs ''before'' overall six clusters).

Plasticity of Connection Rate. The connection rate is characteristic for different microcircuits (17), and, although there are many forms of synaptic plasticity, it is not known whether the connection rate is plastic. We found that, even though connections are spontaneously added and removed, the connection hit rate remained the same over the 12-h period (13.2 ± 0.8%, mean ± SD, $n = 1{,}655$ pairs probed ''before'' vs. 14 ± 2% and 206 pairs probed ''after'' in spontaneous condition). Glutamate application however, caused a massive increase in the overall connection hit rate [29 ± 2% vs. 13.2 ± 0.8%, $n = 354$ pairs probed ''after'' in both evoked conditions pooled and 1,655 pairs probed ''before'' ($P < 0.001$)]. Blocking activity with tetrodotoxin (TTX) prevented the evoked change in the ''after'' connection hit rate (0.5 μM TTX, 13 ± 2%, $n = 228$ pairs probed ''after'').

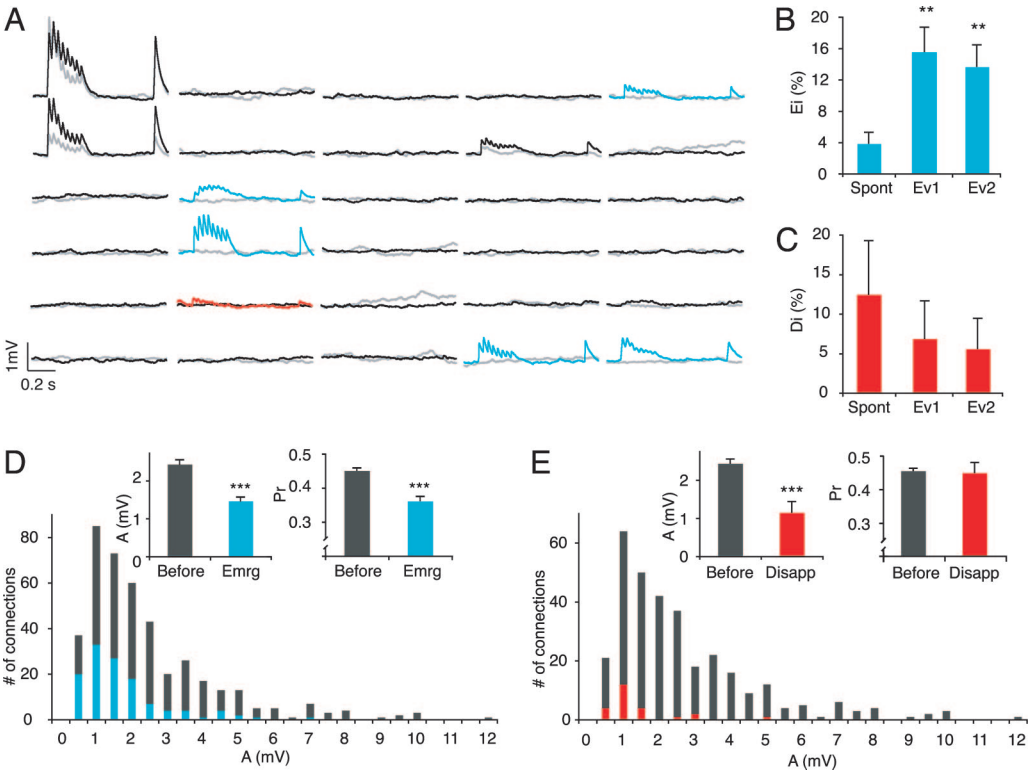

Fig. 2. Spontaneous and evoked emergences and disappearances of connections within 12 h. (*A*) A six-cell cluster showing the EPSPs elicited in response to a train of eight action potentials at 30 Hz and a recovery action potential 500 ms later (average of 30 trials). Each line and column represents a cell. Gray and red traces were recorded at first patch (''before''), and black and blue traces were recorded 12 h later (''after'') under Evoked 1 condition. The red trace indicates a disappearance, and blue traces indicate emergences. (*B*) *Ei* (no. of pairs newly connected ''after''/(no. of unconnected pairs ''before'') for spontaneous ($n = 182$), Evoked 1 (Ev1) ($n = 135$), and Evoked 2 (Ev2) ($n = 154$) conditions (**, $P < 0.001$). (*C*) *Di* (no. of pairs connected ''before'' that were not connected anymore ''after''/(no. of connected pairs ''before'') for spontaneous ($n = 24$), Ev1 ($n = 29$), and Ev2 ($n = 36$) conditions. (*D*) Cumulative distributions of absolute synaptic efficacy (*A*) for recordings at first patch (gray) and emergences (blue) ($n = 322$ and 122, respectively; ***, $P < 0.001$). (*Insets*) Bar graphs of *A* and *Pr* for the same data. (*E*) Same as in *D* but for disappearances (red) ($n = 322$ and 24, respectively; ***, $P < 0.001$).

Obeying Nuclear Recurrence. Connections are also normally formed in a biased manner in that if a neuron receives a connection then the targeted neuron will reciprocate with an even higher connection hit rate (9). This biased connectivity is referred to as ''nuclear recurrence,'' which can be defined as a higher probability of reciprocal connections than the unidirectional connection rate for the circuit. We confirm that, for these neurons, this conditional hit rate is three to four times higher than the unidirectional connection hit rate ($37 \pm 3\%$, $n = 223$ connected pairs ''before''). Even though the mechanism for this reciprocity preference is not known, we did examine whether glutamate-evoked emergence of connections adheres to this biased connectivity rule. Although glutamate application nearly doubled the number of connections, the conditional hit rate for reciprocating connections remained remarkably similar ($37 \pm 5\%$, $n = 104$ connected pairs ''after''), suggesting that the addition of new connections obeys the nuclear recurrence rule by adding proportionally more reciprocal connections than unidirectional ones.

Pharmacology of Microcircuit Plasticity. We next began to study the mechanisms that enable microcircuit plasticity. Blocking action potential activity with TTX caused a significant reduction in evoked emergences [$Ei = 6 \pm 2\%$, $n = 209$ unconnected pairs in six clusters, compared with Evoked 1, $Ei = 16 \pm 3\%$, $n = 135$ unconnected pairs in five clusters ($P < 0.05$)] (Fig. 3*B*) toward spontaneous levels ($Ei = 4 \pm 1\%$, $n = 182$ unconnected pairs in six clusters). Glutamate-evoked emergences therefore depend on action potential activity, but a component still does not. Such activity-independent emergences may account for the spontaneous ones in the quiescent slice and may be due to a tendency for synapse formation in development (21) and in slices (7). Although a strong trend was observed, antagonizing the AMPA receptors [20 μM 6-cyano-7-nitroquinoxaline-2,3-dione (CNQX), $Ei = 9 \pm 2\%$, $n = 166$ pairs in six clusters] or blocking the NMDA receptors [20 μM D-2-amino-5-phosphonopentanoic acid (AP5), $Ei = 13 \pm 3\%$, $n = 159$ pairs in six clusters] did not significantly block the evoked emergences (Fig. 3*B*). Blocking the group 3 [20 μM (*RS*)-α-cyclopropyl-4-phosphonophenylglycine (CPPG), $Ei = 12 \pm 3\%$, $n = 126$ pairs in four clusters] and group 2 [100 μM (2*S*)-α-ethylglutamic acid (EGLU), $Ei = 14 \pm 4\%$, $n = 88$ pairs in three clusters] metabotropic receptors also did not block evoked emergences of new connections (Fig. 3*B*). However, antagonizing the group I metabotropic glutamate receptors (mGluRs) [100 μM DL-2-amino-3-phosphopropinionic acid (AP3), $Ei = 10 \pm 5\%$, $n = 42$ pairs in three clusters], showed a strong tendency to block the emergences, and the specific mGluR5 antagonist [4 μM 2-methyl-6-(phenylethynyl)pyridine (MPEP), $Ei = 7 \pm 2\%$, $n = 162$ pairs in six clusters] caused a significant reduction in evoked emergences toward spontaneous levels [compared with Evoked 1, $Ei = 16 \pm 3\%$ ($P < 0.05$)] (Fig. 3*B*). Detailed measures for the Evoked 1, TTX, and MPEP conditions are given in Table 1. These results indicate that glutamate excitation can drive the formation of new connections in a spiking and mGluR5-dependent manner.

We present the pharmacological experiments also for disappearances, but statistical analysis is not valid because the data set would need to be ≈10 times larger (based on statistical extrap-

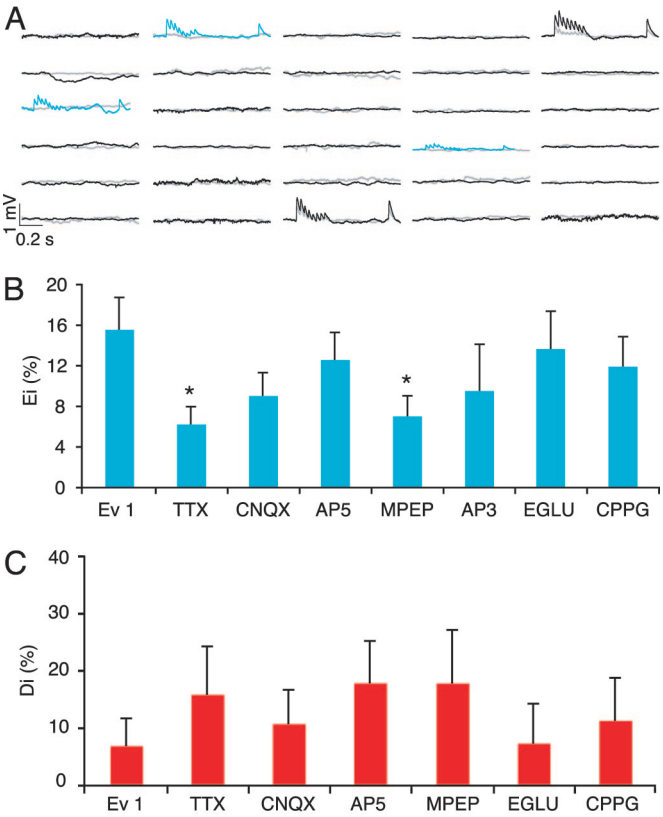

Fig. 3. Emergences depend on mGluR5 and cell action potential activity. (*A*) Six cells cluster EPSPs during continuous MPEP perfusion. (*B*) Bar graphs of the antagonist effects on *Ei* (*, $P < 0.05$). TTX, $n = 209$; CNQX, $n = 166$; AP5, $n = 159$; MPEP, $n = 162$; AP3, $n = 42$; EGLU, $n = 88$; CPPG, $n = 126$. (*C*) Bar graph of the antagonist effects on *Di*. TTX, $n = 19$; CNQX, $n = 28$; AP5, $n = 28$; MPEP, $n = 14$; AP3, $n = 10$; EGLU, $n = 14$; CPPG, $n = 18$.

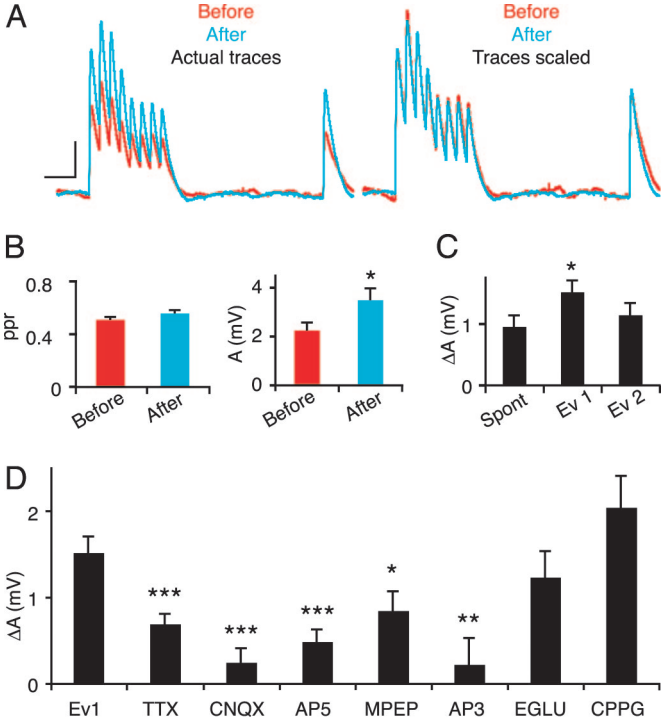

Fig. 4. Spontaneous and induced changes in existing synapses. (*A*) Same EPSP response as in Fig. 2*A*. (*Left*) Comparison of the raw traces at first recording (red) and 12 h later (blue). (*Right*) The same traces but with the first EPSP of the train scaled. The change is only in strength and not in dynamics. (Calibration: 10 ms and 0.5 mV.) (*B*) Bar graphs of the paired-pulse ratio (ppr) (*Left*) and *A* (*Right*) showing that the dynamics is constant and the strength varies over 12 h ($n = 34$ and 40 respectively; *, $P < 0.05$). (*C*) Variation of *A* in 12 h. Spontaneous, $n = 41$; Evoked 1 (Ev1), $n = 63$; Evoked 2 (Ev2), $n = 47$. (*D*) Antagonist effects on *A* variation when glutamate is puffed. TTX, $n = 19$; CNQX, $n = 39$; AP5, $n = 44$; MPEP, $n = 19$; AP3, $n = 14$; EGLU, $n = 21$; CPPG, $n = 37$.

olation from our data). TTX tends to bring disappearances back to spontaneous levels, but the effect was not statistically significant (Fig. 3*C*). Blocking group I mGluRs, but not mGluR5, tends to accelerate evoked disappearances, but the effect was also not statistically significant (Fig. 3*C*). We were unable to track the activity in each neuron for the entire period, so we do not yet know the precise activity patterns driving the switching on and off of connections.

Slow LTP at Existing Connections. We were surprised that NMDA receptors were not required for the rewiring of the circuit and we therefore also examined the changes that occurred at existing connections over this period (between the "before" recording and "after"). Whereas individual connections displayed slower, faster, or no changes in the rates of synaptic depression (*D*), the average changes in dynamics were unaffected, as could be seen by normalizing the responses to the first EPSP (Fig. 4*A*). There was also no average change in the paired-pulse ratio [0.51 ± 0.02 vs. 0.56 ± 0.03, mean $\pm$ SEM ($P = 0.14$), $n = 34$ connections in control experiment] (Fig. 4*B Left*). The change that did occur spontaneously over the 12-h period was that synapses became $\approx$55% stronger [*A* (the absolute efficacy calculated with the Tsodyks–Markram model; see *Materials and Methods*) $= 2.3 \pm 0.3$ mV vs. 3.5 ± 0.5 mV, $n = 40$ connections in control experiment] (Fig. 4*B Right*), as indicated by the uniform change in all responses during the train (Fig. 4 *A* and *B*). This potentiation could be due to the up-scaling of synaptic strength by addition of postsynaptic receptors, when synaptic input is reduced (22). We additionally found that the evoked protocol produced a large and significant additional increase compared with spontaneous changes [$\Delta A = 1 \pm 0.2$ mV (Spontaneous) and 1.5 ± 0.2 mV (Evoked 1), $n = 41$ and 63 connections, respectively, which persisted from "before" to "after"] (Fig. 4*C*), and

Table 1. Detailed measures for the emergences in Evoked 1, TTX, and MPEP conditions

Condition	No. of clusters	No. of patched cells per cluster	No. of connected pairs per cluster		No. of new connections per cluster
			"Before"	"After"	
Evoked 1	5	5, 6, 7, 7, 6	4, 3, 8, 2, 12	5, 7, 13, 9, 14	1, 4, 6, 8, 2
TTX	6	6, 7, 6, 7, 7, 7	1, 2, 5, 6, 2, 3	4, 3, 6, 7, 4, 5	3, 1, 2, 2, 3, 2
MPEP	6	4, 6, 7, 6, 7, 5	2, 4, 3, 0, 3, 2	2, 5, 7, 3, 3, 2	1, 1, 4, 3, 1, 1

The lists give the values for each cluster.

that blocking action potential discharging with TTX and AMPA receptor antagonists prevented this induced change ($\Delta A = 0.7 \pm 0.1$ and 0.2 ± 0.2 mV, $n = 19$ and 39, respectively) (Fig. 4*D*). This slow form of long-term potentiation (sLTP) also depended on NMDA receptor activation ($\Delta A = 0.5 \pm 0.1$ mV, $n = 44$) (Fig. 4*D*) and on the activation of mGluR5 receptors ($\Delta A = 0.8 \pm 0.2$, $n = 19$) (Fig. 4*D*), but not on group II mGluRs ($\Delta A = 1.2 \pm 0.3$, $n = 21$). There was a tendency for greater sLTP when group III mGluRs were blocked ($\Delta A = 2.0 \pm 0.4$, $n = 37$) (Fig. 4*D*). The involvement of spiking activity as well as mGluR5 receptor activation in both the formation and strengthening of connections could imply some overlap in the mechanisms of these two phenomena.

Discussion

We provide direct evidence for a novel form of rewiring plasticity where entire synaptic connections, made up of multiple contacts, are switched on and off over a time scale of hours. Although a component of these changes may be due to ongoing developmental changes and deafferentation caused by the slicing of the tissue, by far the greatest effect is the induced formation of new connections by glutamate excitation in a manner that depends on spiking and mGluR5 activation. We also demonstrate for the first time that the connection rate between neurons is plastic, revealing a novel mechanism to dynamically alter network behavior. We additionally found evidence to suggest that weak connections are preferentially removed, which could explain the presence of strong multisynaptic connections between a small fraction of neurons in the microcircuit. This rewiring of the neocortical microcircuit could occur by conversion of the existing axodendritic close appositions into synapses and vice versa.

The extracellular glutamate concentration *in vivo* is ≈ 10 μM, whereas it can reach 1–10 mM in the cells (23–25) and 1.1 mM in the synaptic cleft (26). The artificial cerebrospinal fluid (ACSF) used in our experiments does not contain any glutamate. Although this is clearly an artificial excitation of the microcircuit, the amount of glutamate, added either by continuous perfusion or by puffing from a distance above the slice, was calibrated to produce moderate discharge responses by the neurons (as indicated in Fig. 1) and is therefore likely to be within physiological ranges. The manner in which activity, mGluRs, and the precise signaling cascade work to set up the signals to connect, not to connect, to remain connected, or to disconnect now requires further study. These changes may be particularly marked at this age of the neocortex because this is the period during which the first decisions are being made by neurons to choose their synaptic partners. We did attempt to carry out these experiments in adult slices, but these slices do not survive such long-lasting experiments in our experimental conditions. However, it is worth pointing out that, at this age, the axonal and dendritic arborizations have already elaborated to such an extent that all axons are able to be in close apposition with all dendrites multiple times (4, 5), which is most likely the essential substrate for microcircuit plasticity. In other words, a major component of microcircuit plasticity requires that the microcircuit has reached a minimal level of axonal and dendritic arborization.

This study shows that, after activity is evoked with glutamate application, the connection rate can increase >3-fold. It is unlikely that experience would continuously drive the rate up during the life of the animal. Indeed, these neurons in the adult somatosensory cortex have basically the same hit rate as in the 2-week-old rat [10–15% (15) in 3-month-old rats; T. Berger, G. Silberberg, and H.M., unpublished observations]. It is therefore more likely that the burst of new connections induced by a new stimulus is a transient process due to an imbalance between the formation of new and the removal of existing connections. Indeed, there was a trend to prevent removal of connections after the evoked activity. If the connection rate is to return to control levels after such activity, the rate of removal of connections would need to rise with a significant delay after the increase in the emergence of new connections.

We therefore speculate that a sequence of events is triggered by new experiences (a burst of many new connections in the network with more synapses added per connection over time, a window of grace for the new low-probability connections to be tested for their improved value in processing the new environment, an elimination process), which removes the weakest connections and reestablishes the connection rate characteristic for the microcircuit. Such a process could be analogous to a burst of mutations in a species caused by major environmental change followed by natural selection of the most adapted variants. We therefore speculate that microcircuit plasticity may allow neural networks to continue the evolutionary process in a Darwinian manner as a function of experience (see also ref. 27).

Materials and Methods

Electrophysiological Recordings. Young (postnatal day 12–14) Wistar rats were rapidly decapitated, and their brains were removed and sliced in an ACSF containing 125 mM NaCl, 2.5 mM KCl, 25 mM D-glucose, 25 mM $NaHCO_3$, 1.25 mM NaH_2PO_4, 2 mM $CaCl_2$, and 1 mM $MgCl_2$. The sagittal somatosensory cortex brain slices were then perfused with 35°C ACSF for the whole experiment. Somatic multiple whole-cell recordings were made, and signals were amplified by using Axoclamp-200B amplifiers (Axon Instruments, Union City, CA) and digitized by means of an ITC-18 interface (Instrutech, Great Neck, NY) to an Apple computer running Igor Pro (Wavemetrics, Portland, OR). Voltages were recorded with pipettes containing 100 mM potassium gluconate, 10 mM KCl, 4 mM ATP-Mg, 10 mM phosphocreatine, 0.3 mM GTP, 10 mM Hepes, and 5 mg·ml^{-1} biocytin (pH 7.3, 310 mosmol·liter^{-1}, adjusted with sucrose). The pipettes were pulled with Flaming/Brown micropipette puller P-97 (Sutter Instruments, Novato, CA). All animal experiments were done under the authorization no. 1550 of the Service Vétérinaire de l'Etat de Vaud.

Clusters of six to seven TPCs were patched a first time ("before"), and their connectivity was recorded by using, successively, for each cell, a train of eight action potentials at 30 Hz followed by a recovery test spike 500 ms later. The stimulation was repeated 30 times, and the averaged trace was used for analysis. Recordings were obtained ≈ 2 h after slicing in an attempt to avoid the initial increase in synapses reported because of slicing (7). Within 20 min the pipettes were withdrawn, and the slice was left in the recording chamber with various conditions. For the spontaneous condition, we continued perfusing only ACSF. Evoked 1 was ACSF in the presence of puffs of 50 mM sodium glutamate 100 μm above the cell cluster (Fig. 1 *C* and *D*). Evoked 2 was ACSF perfused with 100 μM sodium glutamate (Sigma-Aldrich, St. Louis, MO) (Fig. 1*E*). The various antagonist conditions correspond to the slice perfused with ACSF containing the antagonist concentrations described below and glutamate puffing on the cluster.

The monitor display from the Axioskop (Zeiss, Jena, Germany) and charge-coupled device camera (Hamamatsu, Hamamatsu City, Japan) were used to capture IR differential interference contrast images, define landmarks, and find the same cell cluster 12–14 h later (Fig. 1*A*). The microscope focus on the cells was also maintained throughout the experiment. The cells were then repatched, and the same stimulation protocol was executed to monitor the connectivity in the new state ("after"). After recording, the slices were fixed and ABC-stained, and, because biocytin was used in the first and second patchings, we could double-check that the same cluster was patched for each experiment (Fig. 1*B*). In one case, when the IR differential interference contrast localization of the cluster was not convinc-

ing, two clusters were clearly seen corresponding to the "before" and "after" patching sessions. This finding shows that the biocytin is preserved in the cell even after >12 h in the recording chamber.

The electrophysiological responses were analyzed off-line (Igor), and the Tsodyks–Markram model was used on the averaged traces to determine synaptic properties. The model yields the absolute synaptic efficacy (A) that is the total amount of resources the unperturbed presynaptic neuron has over all of its synapses (expressed in millivolts measurable in the postsynaptic neuron). It then also yields the utilization of synaptic efficacy (ranged between 0 and 1), which is the fraction of the resources used by one action potential. The EPSP size is the product of A with the utilization of synaptic efficacy. Because A is the total amount of resources and the depression in TPCs is mostly presynaptically mediated (28, 29), A is equivalent to the number of release sites multiplied by the quantum size. The EPSP size is then A multiplied by the Pr. Consequently, the utilization of synaptic efficacy is equivalent to the Pr, which is then derived directly from the fitting of the model on the averaged traces.

The condition of slices at 12 h was excellent (Fig. 1*A*), with high visibility, no change in patchability (reflection of slice health), normal break-in resting potentials, normal discharge behavior, and no change in input resistances.

Histological Procedure. After the recording, the 300-μm slices were fixed for at least 24 h in a cold 0.1 M phosphate buffer (100 mM, pH 7.4) containing 2% paraformaldehyde and 1% glutaraldehyde. Thereafter, the slices were rinsed and then transferred into a phosphate-buffered 3% H_2O_2 to block endogenous peroxidases. After rinsing in the phosphate buffer, slices were incubated overnight at 4°C in an avidin-biotinylated horseradish peroxidase (ABC-Elite; Vector Laboratories; 2% A, 2% B, and 1% Triton X-100). Subsequently, sections were rinsed again in the phosphate buffer and developed with diaminobenzidine under visual control by using a bright-field microscope (Axioskop) until processes of the cells were clearly visible. Finally, the reaction was stopped by transferring the sections into the phosphate buffer. After rinsing in the phosphate buffer, slices were mounted in an aqueous mounting medium.

Pharmacology. The following pharmacological agents were used: 0.5 μM TTX, a sodium channel blocker (Alomone Labs, Jerusalem, Israel); 20 μM CNQX, an α-amino-3-hydroxy-5-methyl-4-isoxazolepropionic acid receptor antagonist (Sigma-Aldrich); 20 μM AP5, an *N*-methyl-D-aspartic acid receptor antagonist (Tocris, Ellisville, MO); 4 μM MPEP, an mGluR5 antagonist (Tocris); 100 μM AP3, a group I mGluR antagonist (Tocris); 100 μM EGLU, a group II mGluR antagonist (Tocris); and 20 μM CPPG, a group III mGluR antagonist (Tocris).

Statistical Tests. Student t tests were used on the Gaussian-like distributions such as the distribution of the Pr, the paired-pulse ratio distributions, the changes in A, and the natural logarithm of A"before" vs. A"after." The comparison of A"before" and A"after" was made with a Kolmogorov–Smirnov test. The proportion of emergences and disappearances and the proportion of reciprocal emergences were tested by using the χ^2 test. Because the connection hit rates and the proportions of emergences and disappearances were estimated as being the proportion of connections observed in the respective conditions (as opposed to the number of connections not observed, i.e., not present, not emerged, or not disappeared), the standard deviations were calculated on the base of a binomial distribution: $SD = \sqrt{(p(1-p)/n)}$.

Indices and Formulations. The Ei was calculated as follows: Ei = (no. of connections that emerged)/(no. of remaining possible connections) where (no. of remaining possible connections) = (no. of pairs) − (no. of connections at first recording).

The Di was calculated as follows: Di = (no. of connections that disappeared)/(no. of connections at first recording).

The CV of a connection was calculated by measuring the amplitude of the first EPSP of the 30-Hz train for each of the 30 trials. The standard deviation of these 30 amplitudes was calculated. CV is the standard deviation divided by the mean of the 30 amplitudes.

For a given number of synapses N in a connection, the expected CV can be calculated by using the binomial assumption $N = (1 - Pr)/(Pr\,CV^2)$ and knowing the Pr. Knowing the Pr for connection 1 (Pr_1) and both the Pr and the CV for connection 2 (Pr_2 and CV_2), the CV for the connection 1 can be derived (CV_1) assuming the same number of synapses for both connections: $CV_1 = CV_2\ \sqrt{[(1 - Pr_1)Pr_2]/[(1 - Pr_2)Pr_1]}$. The comparison between the predicted value of CV_1 and the actual value measured gives an indication of the relative number of synapses in both connections. If the actual CV is greater than the predicted, it can be concluded that connection 1 has fewer synapses than connection 2.

The connection hit rate is the number of connections divided by the number of neuron pairs considered, and the conditional reciprocal connection hit rate is the number of neuron pairs reciprocally connected divided by the total number of connected pairs.

1. Wolff, J. R. & Missler, M. (1993) *APMIS Suppl.* **40,** 9–23.
2. Montgomery, J. M. & Madison, D. V. (2004) *Trends Neurosci.* **27,** 744–750.
3. Hensch, T. K. (2005) *Nat. Rev. Neurosci.* **6,** 877–888.
4. Kalisman, N., Silberberg, G. & Markram, H. (2005) *Proc. Natl. Acad. Sci. USA* **102,** 880–885.
5. Chklovskii, D. B., Mel, B. W. & Svoboda, K. (2004) *Nature* **431,** 782–788.
6. Morishima, M. & Kawaguchi, Y. (2006) *J. Neurosci.* **26,** 4394–4405.
7. Kirov, S. A., Sorra, K. E. & Harris, K. M. (1999) *J. Neurosci.* **19,** 2876–2886.
8. Markram, H., Lubke, J., Frotscher, M., Roth, A. & Sakmann, B. (1997) *J. Physiol. (London)* **500,** 409–440.
9. Markram, H. (1997) *Cereb. Cortex* **7,** 523–533.
10. Bienenstock, E. (1996) *J. Physiol. (Paris)* **90,** 251–256.
11. Thomson, A. M. & Bannister, A. P. (2003) *Cereb. Cortex* **13,** 5–14.
12. Sjostrom, P. J., Turrigiano, G. G. & Nelson, S. B. (2001) *Neuron* **32,** 1149–1164.
13. Markram, H. & Tsodyks, M. (1996) *Nature* **382,** 807–810.
14. Markram, H., Lubke, J., Frotscher, M. & Sakmann, B. (1997) *Science* **275,** 213–215.
15. Thomson, A. M., West, D. C., Wang, Y. & Bannister, A. P. (2002) *Cereb. Cortex* **12,** 936–953.
16. Holmgren, C., Harkany, T., Svennenfors, B. & Zilberter, Y. (2003) *J. Physiol. (London)* **551,** 139–153.
17. Watts, J. & Thomson, A. M. (2005) *J. Physiol. (London)* **562,** 89–97.
18. Feldmeyer, D. & Sakmann, B. (2000) *J. Physiol. (London)* **525,** 31–39.
19. Redman, S. (1990) *Physiol. Rev.* **70,** 165–198.
20. Thomson, A. M. (1998) *C. R. Acad. Sci. III* **321,** 131–133.
21. Lendvai, B., Stern, E. A., Chen, B. & Svoboda, K. (2000) *Nature* **404,** 876–881.
22. Turrigiano, G. G. & Nelson, S. B. (2000) *Curr. Opin. Neurobiol.* **10,** 358–364.
23. Danbolt, N. C. (2001) *Prog. Neurobiol.* **65,** 1–105.
24. Erecinska, M. & Silver, I. A. (1990) *Prog. Neurobiol.* **35,** 245–296.
25. Chen, Y. & Swanson, R. A. (2003) *J. Cereb. Blood Flow Metab.* **23,** 137–149.
26. Clements, J. D., Lester, R. A., Tong, G., Jahr, C. E. & Westbrook, G. L. (1992) *Science* **258,** 1498–1501.
27. Edelman, G. M. (1993) *Neuron* **10,** 115–125.
28. Tsodyks, M., Pawelzik, K. & Markram, H. (1998) *Neural Comput.* **10,** 821–835.
29. Thomson, A. M., Deuchars, J. & West, D. C. (1993) *J. Neurophysiol.* **70,** 2354–2369.